Iron-boron pairing kinetics in illuminated p-type and in boron/phosphorus co-doped n-type silicon

Christian Möller,[1,2,a)] Til Bartel,[3] Fabien Gibaja,[3] and Kevin Lauer[1]
[1]*CiS Forschungsinstitut für Mikrosensorik und Photovoltaik GmbH, Konrad-Zuse-Str. 14, 99099 Erfurt, Germany*
[2]*TU Ilmenau, Institut für Physik, Weimarer Str. 32, 98693 Ilmenau, Germany*
[3]*Calisolar GmbH, Magnusstraße 11, 12489 Berlin, Germany*

(Received 29 April 2014; accepted 26 June 2014; published online 10 July 2014)

Iron-boron (FeB) pairing is observed in the n-type region of a boron and phosphorus co-doped silicon sample which is unexpected from the FeB pair model of Kimerling and Benton. To explain the experimental data, the existing FeB pair model is extended by taking into account the electronic capture and emission rates at the interstitial iron (Fe_i) trap level as a function of the charge carrier densities. According to this model, the charge state of the Fe_i may be charged in n-type making FeB association possible. Further, FeB pair formation during illumination in p-type silicon is investigated. This permits the determination of the charge carrier density dependent FeB dissociation rate and in consequence allows to determine the acceptor concentration in the co-doped n-type silicon by lifetime measurement. © *2014 AIP Publishing LLC*. [http://dx.doi.org/10.1063/1.4889817]

I. INTRODUCTION

Iron is one of the most investigated transition metal impurities in silicon. This investigation started in the late 1950s with the work of Collins and Carlson.[1] They proved that the donor level discovered in iron contaminated silicon is indeed the level of interstitial iron (Fe_i). A review on iron and its complexes in silicon was given by Istratov *et al.*[2] They specified more precisely the donor level of Fe_i with $E_v + 0.38\,eV$. First experimental evidence of an iron-boron pairing reaction in silicon was published by Shepherd and Turner in 1962.[3] The acceptor level of the iron-boron (FeB) pair was determined by Rein and Glunz[4] to $E_c - 0.26\,eV$. Kimerling and Benton introduced a Fermi level dependent FeB kinetic model,[5] based on the iron related energy states in the silicon band gap.

In this paper, the understanding of the FeB association kinetics is extended by a dynamic approach. It relates the charge carrier capture and emission rates of the Fe_i and FeB trap levels with the FeB association and dissociation rates. This model allows to explain the FeB pairing kinetics, observed in boron and phosphorus co-doped n-type silicon. First, the FeB pairing model is introduced (Sec. II). Experimental details are given in Sec. III. The FeB pairing reaction observed in co-doped n-type silicon and during illumination in boron-doped samples is presented in Sec. IV. Finally, the experimental results are discussed in Sec. V.

II. IRON-BORON PAIRING MODEL

A. The conventional FeB pairing model

Due to its high mobility, Fe_i is able to diffuse through the silicon lattice at room temperature. Depending on its charge, Fe_i forms pairs with negatively ionized acceptors. The pair formation happens for a p-type sample left at room temperature in darkness. FeB pairs can be dissociated by illumination,[6] minority carrier injection[5] and thermal treatment at 200 °C.[6]

In the conventional FeB model, the Fermi level position determines the ability of Fe_i to pair with an acceptor: If the Fermi level is located between the Fe_i energy level ($E_v + 0.38\,eV$[2]) and the boron energy level ($E_v + 0.045\,eV$[5]), the interstitial iron is charged positively (Fe_i^+) and the substitutional boron negatively (B_S^-). As a consequence, pairing occurs (Fig. 1(a)). If the Fermi level exceeds the Fe_i energy level, interstitial iron becomes neutral and no association is expected.[5] The stability condition for the FeB pairs as a function of the Fermi level position is depicted by the shaded area in Fig. 1(b). Once created, FeB pairs are expected to remain stable until the Fermi level exceeds the acceptor FeB level at $E_c - 0.26\,eV$.[4] Now, the $Fe_i^+B^-$ captures an electron that neutralizes the interstitial iron. The Coulombic attraction disappears and the Fe_i^0 unbinds from the B_S^- and can again diffuse through the silicon crystal.[2]

B. Dynamic FeB pair model

To explain the experimental findings presented in Sec. IV, it is necessary to extend the existing model. The rate of charge carrier capture and emission by the involved defects states and, consequently, the rates of FeB association and dissociation are taken into account.

During the association process a dynamic reaction between interstitial iron, electrons, holes and boron occurs until a steady state between FeB dissociation and association is reached. The steady state is dependent on the boron dopant density, the charge carrier densities and temperature. A diagram of the processes involved in the FeB pair reaction is shown in Fig. 2. For the positively charged Fe_i^+, two possible reactions exist: In the first case, the Fe_i^+ captures an electron and becomes neutral (Fe_i^0). The Fe_i^0 can capture a hole and becomes Fe_i^+ again. The second possibility is the field

a)Author to whom correspondence should be addressed. Electronic mail: cmoeller@cismst.de

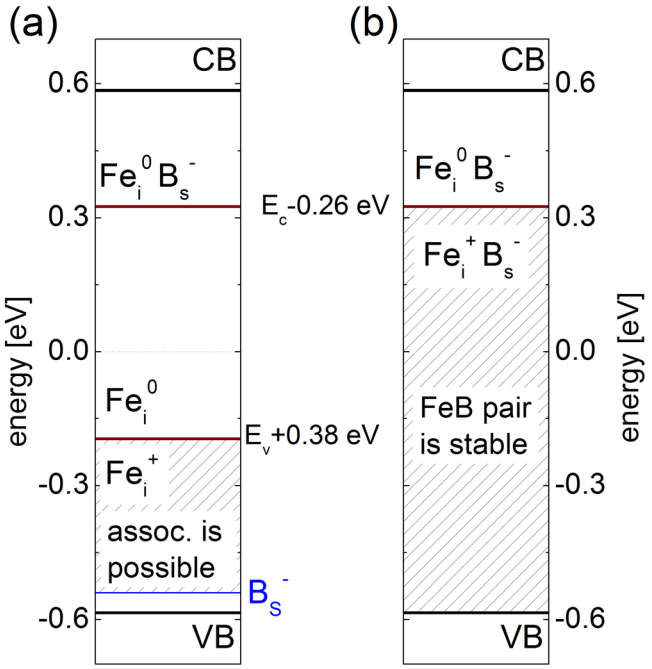

FIG. 1. Fermi level dependent stability of FeB pairs in the silicon band-chart.[5] The shaded areas denote the Fermi level region in which (a) association of FeB takes place and (b) FeB pairs are stable. Dissociation occurs if the Fermi level exceeds the FeB level $E_c - 0.26\,\text{eV}$.

assisted migration of the Fe_i^+ towards the negatively charged substitutional boron (B_S^-) due to the Coulombic attraction and $Fe_i^+B_S^-$ pair formation. Which reaction path of Fe_i prevails, depends on its charge state, the concentration of charge carriers and boron atoms (at a given temperature).

$Fe_i^+B_S^-$ on the other hand may dissociate. The final equilibrium between free Fe_i^0 and $Fe_i^+B_S^-$ is determined by the following rate equations:

$$\begin{aligned} Fe_i^+ + B_S^- &\xrightarrow{k_A} Fe_i^+B_S^- \\ Fe_i^+B_S^- &\xrightarrow{k_D} Fe_i^0 + B_S^-, \end{aligned} \tag{1}$$

where k_A and k_D are the association and dissociation rates of the FeB pairs, respectively.

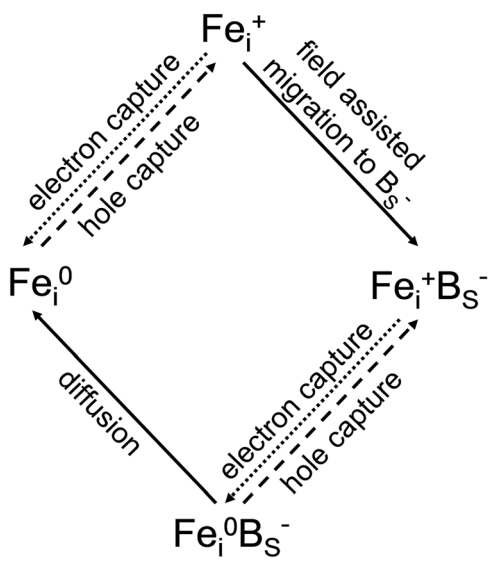

FIG. 2. Reaction paths in the dynamic iron-boron pairing model.

The dissociation process of FeB pairs by electron capture was discussed by Kimerling and Benton.[5] They concluded that an electron capture process leads to a neutralization of the Fe_i^+ which removes the Coulombic attraction between Fe_i^0 and boron. But this neutralization is not sufficient to result in a spatial dissociation at room temperature because experimentally an $E = 0.8\,\text{eV}$ Fe_i^0 diffusion barrier was detected.[7] In the literature, two possibilities of energy deposition are discussed:[8] a second electron capture of the Fe_i^0 which leads to a negative charge state (Fe_i^-) and consequently to a Coulombic repulsion of the $Fe_i^-B_S^-$ pair and a second electron capture depositing the necessary Fe_i^0 migration energy after recombination with a hole. The energy deposition by recombination is known as recombination-enhanced defect reaction (REDR) and is caused by strong electron-lattice coupling at the defect.[9–11]

III. EXPERIMENTAL DETAILS

Sample information is given in Table I. The ingot from which sample D was taken was produced from electronic grade silicon. Crystallization started with 0.5 ppmwt boron and 2.4 ppmwt phosphorus in the melt.

The samples were contaminated with iron when necessary as described in Refs. 12–14. Before lifetime measurement, all samples were RCA cleaned and surface passivated by a PECVD nitride layer.[15] To exclude the light-induced degradation defect during illumination dependent lifetime measurements, all samples were illuminated for 48 h at room temperature.

The FeB pair association kinetics were monitored by lifetime measurements with a Semilab WT-2000 microwave-detected photoconductance decay (MWPCD) device. The lifetime of the excess minority charge carriers was calculated from the MWPCD signal at an excess charge carrier density of $\Delta n = 5 \times 10^{14}\,\text{cm}^{-3}$, calibrated by comparison with a quasi-steady-state photoconductance decay (QSSPC)[18] measurement.[19] The laser (200 ns pulse, wavelength 904 nm) dissociates the FeB pairs during the continuous lifetime measurement and no additional illumination is needed. The MWPCD halogen bias light was used to illuminate the p-type samples. The illumination intensity of the MWPCD bias light, at the used measurement distance of 0.8 mm from the sample surface, was determined with a calibrated reference cell. During the lifetime measurement, the bias light was switched off to measure the effective lifetime instead of the differential lifetime.[20] The time without illumination (<1 s) is too short for a measurable association of the FeB pairs. The change in the relative interstitial iron content [Fe_i] due to FeB pair dissociation was deduced from the MWPCD lifetime values before and during/after illumination of the sample.[21,25]

IV. EXPERIMENTAL RESULTS

A. FeB pairing kinetics in co-doped n-type silicon

FeB pairing kinetics are monitored in boron- and phosphorus-doped silicon (sample D) in the region in which it is shown to be n-type silicon (proved with hot-probe experiment). Fig. 3 depicts the lifetime map (a) and the

TABLE I. Details of silicon samples used in this study. The lifetime value τ_{FeB} (at $\Delta n = 1 \times 10^{15}\,cm^{-3}$) describes the lifetime in the FeB state. With known carrier mobility,[16] the carrier density and thus the electrically active dopant density was calculated from the four-point-probe resistivity measurement.[17]

	Dopant/crystallization technique	Resistivity [Ωcm]	Dop. conc. [cm^{-3}]	Thickness [μm]	τ_{FeB} [μs]	Interstitial iron content [Fe_i] [cm^{-3}]	Sample size [cm]
A	Boron/mc	1.0	1.5×10^{16}	150	8.2	9.6×10^{12}	2.4×6
B	Boron/CZ	4.0	3.5×10^{15}	180	7.7	9.0×10^{12}	5×5
C	Boron/CZ	11.66	1.2×10^{15}	720	3.9	5.6×10^{12}	5×5
D	Boron, phosphorus/CZ	3.1 p-type to 0.15 n-type (see Fig. 3(b))	see Fig. 8	470	~17.5 (see Fig. 3(a))	6.9×10^{12} [a]	5×14

[a]Changes in the interstitial iron content are discussed in Sec. V C.

height dependent resistivity at three different lateral positions (b) of sample D. Transition from p-type to n-type silicon occurs (x-position dependent) at an ingot height of around y = 5–8 cm (Fig. 3(b)).

The observed reciprocal lifetime characteristic under illumination and in the dark indicates FeB pairing kinetics. With the used measurement conditions other defects like chrome-boron pairs[22] and lifetime change due to copper precipitation[23] are excluded. The FeB pairing kinetics observed by lifetime measurements of three consecutive cycles of FeB pair dissociation and association are shown in Fig. 4. Time dependent minority carrier lifetime was measured at ingot height y = 6.2 cm and x = 1 cm (n-type region, $\rho = 82$ Ωcm). The FeB pair formation kinetics which are usually observed in p-type silicon were also found to occur in phosphorus and boron co-doped silicon which was n-type.

As stated in Sec. II A, the observation of FeB association and dissociation is unexpected in the n-type region of a boron and phosphorus co-doped silicon sample, since Fe_i should remain uncharged and incapable of forming pairs with boron (conventional model Sec. II A). In view of the results, positively charged Fe_i^+ must exist in the n-type region for a sufficient time to produce a measureable FeB formation. To evaluate the probability of such an event at high electron densities as encountered in n-type silicon, electrons are injected in p-type samples by bias illumination. The resulting illumination dependent association kinetics allow an approximation of the same kinetics in the co-doped n-type silicon.

B. FeB association under illumination in p-type silicon

Illumination of p-type silicon leads to an increasing electron density in the conduction band which can help understand the Fe_i reaction paths in co-doped n-type silicon (Fig. 2). The time dependent reciprocal lifetime of p-type samples at different bias light illumination intensities is depicted in Fig. 5.

For injection levels above the cross-over point (lifetime remains unchanged after dissociation), the FeB pair is more recombination active than the Fe_i.[24] Consequently, reciprocal lifetime decreases during dissociation (Fig. 5, black filled symbols). With increasing illumination the steady state reciprocal lifetime decreases as expected for a sample with an increasing unpaired Fe_i population. With no exception to this effect, the reported lifetime variation under bias light illumination is characteristic for the FeB pair reaction and is fully reversible. First, the lifetime increases due to FeB dissociation under strong illumination (black filled symbols in Fig. 5). In darkness (no bias light), FeB pairs form again and the lifetime starting value is fully recovered. With the bias light illuminating the sample, only a fraction of the Fe_i associates again and the reciprocal lifetime saturates at smaller values. With increasing boron-doping density, stronger

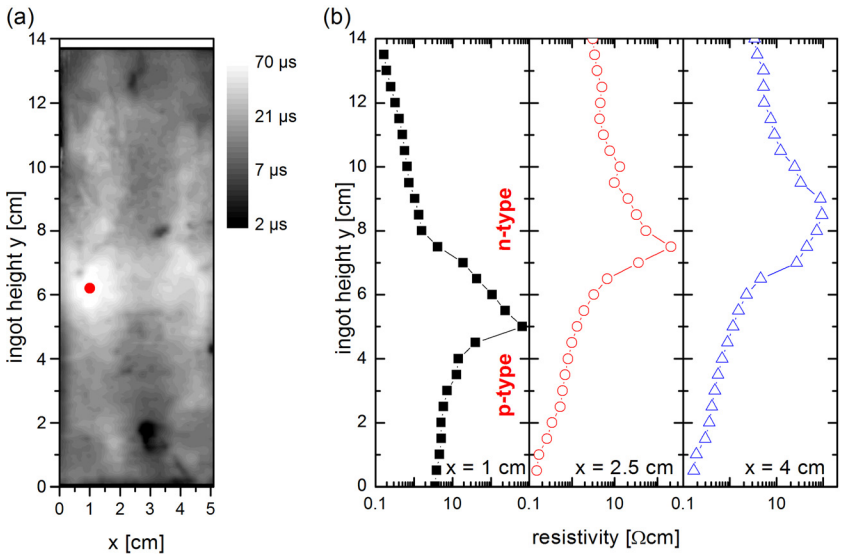

FIG. 3. Data from sample D. (a) Lifetime map of the sample and (b) resistivity at three different x-coordinates. Measurement position of Fig. 4 is depicted in the lifetime map as red dot.

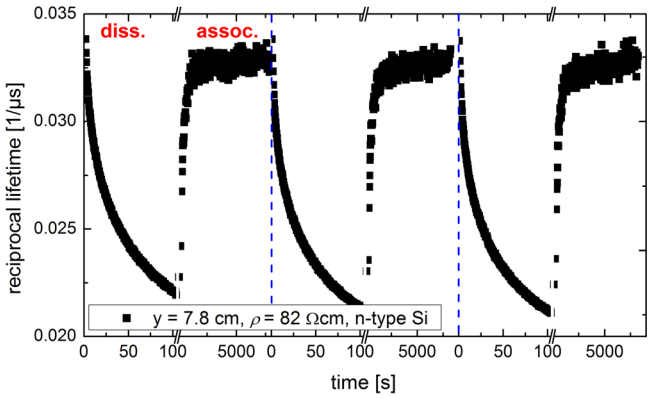

FIG. 4. Lifetime measurement during three consecutive FeB pair dissociation and association cycles in the n-type silicon region of sample D (ingot height y = 6.2 cm and x = 1 cm, depicted in Fig. 3(a) as red dot). Full reversibility of the measurements is visible. In the first cycle, dissociation (diss.) and association (assoc.) are labelled. Note the different time scales for dissociation and association, respectively.

illumination is needed to prevent complete FeB association. Note the different time scales in Fig. 5. The time needed for reaching the lifetime steady state increases with decreasing boron concentration.[25]

V. DISCUSSION

A. Examination of the introduced dynamic approach

The introduced model is based on the interaction between charge state change of the Fe_i and Fe_i migration to boron. This raises several questions. How long is the Fe_i in the positive charge state? Which processes are responsible for the FeB pairing kinetics in boron and phosphorus co-doped n-type silicon presented in Sec. IV A?

The first question can be answered by a simple estimation of the processes p-type silicon under bias light illumination. During illumination the charge carrier recombination rate per Fe_i^+ can be calculated with the capture rates of electrons c_n and holes c_p,

$$c_n = \sigma_n v_{th}\, n = 4.4 \times 10^7\ s^{-1}$$
$$c_p = \sigma_p v_{th}\, p = 2.77 \times 10^6\ s^{-1}. \quad (2)$$

$\sigma_n = 4 \times 10^{-14}\,cm^2$ and $\sigma_p = 7 \times 10^{-17}\,cm^2$ are the capture cross sections for electrons and holes of the Fe_i^+ and the Fe_i^0 trap[2], $v_{th} = 1.1 \times 10^7\,cm/s$ is the thermal velocity, $n = n_0 + \Delta n$ and $p = p_0 + \Delta p$ are the electron and hole densities, respectively. Electron emission out of the Fe_i^0 level is neglected because this process changes the charge state of the Fe_i and, hence, supports the recharge process which leads only to an underestimation of the time in the positive charge state. The given values are calculated for sample B at an illumination induced excess charge carrier density of $\Delta n = \Delta p = 1 \times 10^{14}\,cm^{-3}$ (equals 0.9 sun at $\tau = 10\,\mu s$) at room temperature. The recombination rate per Fe_i^+ is limited by the smallest calculated capture rate Eq. (2). With the assumption that every hole capture leads to a recombination process, a recombination rate of $R_{illum.} = 2.77 \times 10^6\,s^{-1}$ over one Fe_i^+ trap occurs. The reciprocal values of the capture rates specify

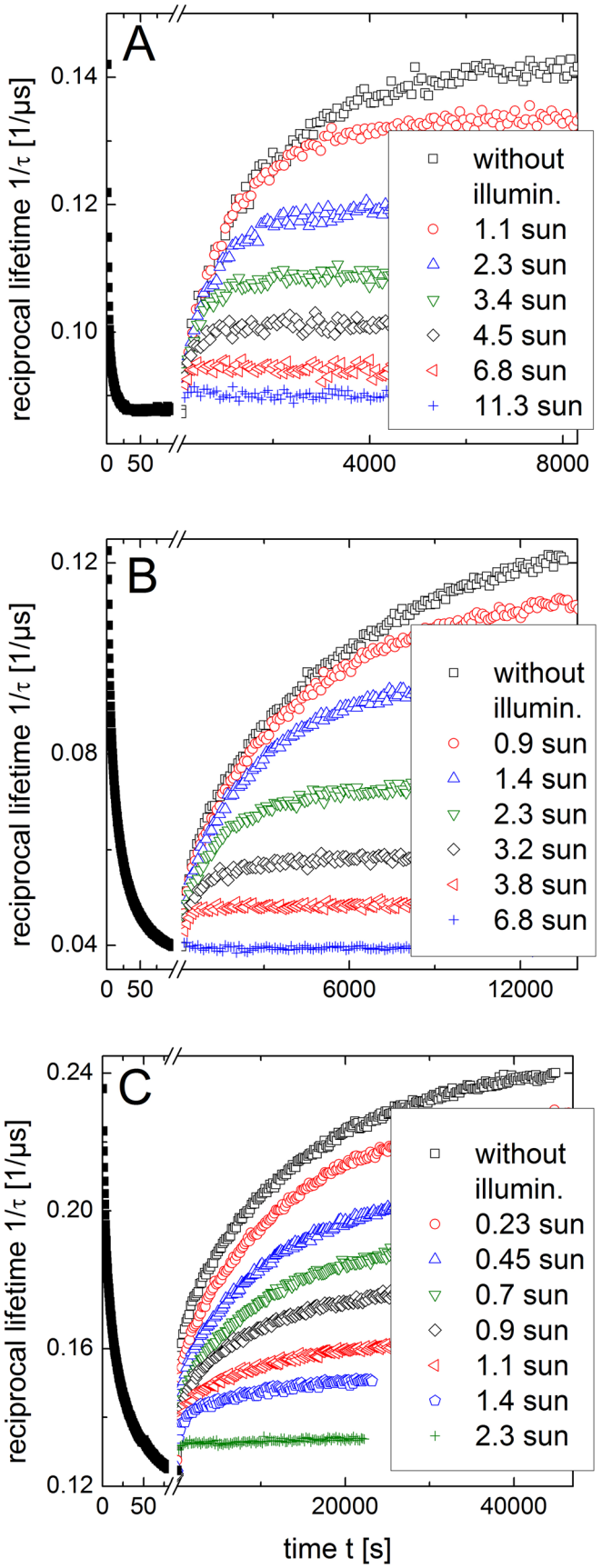

FIG. 5. Time dependent reciprocal lifetime during FeB pair dissociation and association at different bias light illumination intensities of sample A (1.0 Ωcm), B (4.0 Ωcm), and C (11.66 Ωcm). Note the changing illumination intensities and time scales.

the time for capture an electron or a hole. The minimum time in the Fe_i^+ state is calculated with the assumption that the Fe_i^+ first captures an electron and afterwards the hole. This leads, with the given example parameters, to a time ratio of $Fe_i^+/Fe_i^0 = 0.06$. Hence, the diffusing Fe_i experiences weakened Coulombic attraction caused by the permanent switch between Fe_i^0 and Fe_i^+ (about 10^6 times per second). However the association still occurs at the same rate because the attraction to boron still exists. Note that the decreasing reciprocal lifetime with increasing illumination (Fig. 5) is caused by an increasing dissociation rate (discussed in Sec. V B).

FeB association in co-doped n-type silicon is not explainable with the simple estimation done for illuminated p-type silicon. Indeed, the small hole density (with n-type doping $n_0 = 1 \times 10^{14}\,cm^{-3}$ and $p_0 = 1.2 \times 10^6\,cm^{-3}$) leads with Eq. (2) to a negligible charged Fe_i state. To explain FeB association in co-doped n-type silicon the thermal emission of charge carriers out of the occupied Fe_i^0 trap level had to be taken into account. The relation between the emission rates of electrons e_n or holes e_p and the capture rates c_n and c_p in the thermal steady state of one Fe_i trap is given by[26]

$$\frac{e_n}{c_n} = n\frac{1-f_t}{f_t}, \quad \text{with} \quad n = N_C \exp\left[\frac{E_F - E_c}{k_B T}\right] \tag{3a}$$

$$\frac{e_p}{c_p} = p\frac{f_t}{1-f_t}, \quad \text{with} \quad p = N_V \exp\left[-\frac{E_F - E_v}{k_B T}\right]. \tag{3b}$$

N_C and N_V are the effective densities of states in conduction- and valence band, respectively, E_F is the Fermi energy, T the absolute temperature, k_B the Boltzmann-constant, E_c and E_v are the energetic position of the conduction and valence band. The occupation probability of the trap level E_t is given by $f_t = (\exp[\frac{E_t - E_F}{k_B T}] + 1)^{-1}$. From Eq. (3) follows that the emission of excess electrons and holes out of one Fe_i trap state is $e_n/c_n = 9.0 \times 10^6\,cm^{-3}$ and $e_p/c_p = 1.3 \times 10^{13}\,cm^{-3}$. All emitted charge carriers had to be captured again (steady state condition). Hence, the interaction of emission and capture of holes (and electrons) create a permanent charge state change (Fe_i^0 to Fe_i^+) of the Fe_i. These processes occur in thermal steady state and are used for a qualitative description of the association process in n-type silicon.

Dissociation of FeB pairs is an electron-driven process (Sec. II B). Hence the temperature induced dissociation of FeB pairs can be explained by an increase of the thermal generation rate due to annealing. During the annealing step at 200 °C, the intrinsic charge carrier density increases from $n_{i,T=25\,°C} = 1.07 \times 10^{10}\,cm^{-3}$ to $n_{i,T=200\,°C} = 1.11 \times 10^{14}\,cm^{-3}$. This leads to an electron density increase in the conduction band from $n_{25\,°C} = 3.3 \times 10^4\,cm^{-3}$ to $n_{200\,°C} = 3.5 \times 10^{12}\,cm^{-3}$ (at a doping density of $N_A = 3.5 \times 10^{15}\,cm^{-3}$). Based on Eq. (2) and with the capture cross-sections of the FeB trap,[27] the recombination rate per FeB trap increases from $R_{thermal\ 25\,°C} = 9.1 \times 10^{-4}\ s^{-1}$ at room temperature to $R_{thermal\ 200\,°C} = 9.6 \times 10^4\,s^{-1}$. The increasing thermal generation rate induces an increased probability of the electron capture, which leads to the dissociation due to consecutive electron capture of the FeB pairs.

B. Association rate and dissociation rate

The measurements on illuminated p-type silicon show that FeB pairing occurs with increasing electron density as well. Based on the illumination dependent measurements in p-type silicon, the interaction of dissociation- and association rate can be determined and transferred to n-type silicon.

The reciprocal lifetime values, depicted in Fig. 5, were calculated into the time dependent relative interstitial iron content $[Fe_i]_{relative}$ described in Sec. III. After complete association, the $[Fe_i]_{relative}$ equals zero: all interstitial iron is bound in FeB pairs. The value one depicts the point where all FeB pairs are dissociated. In Fig. 6, the $[Fe_i]_{relative}$ is exemplarily shown in dependence of the illumination intensity of sample B. With increasing illumination intensity the amount of interstitial iron increases. Hence, the amount of associated FeB pairs decreases. With increasing boron-doping density, the illumination intensity has to increase to prevent the FeB association completely (Fig. 5). This is caused by the reduced boron spacing which increases the association rate. Hence, a higher electron density is necessary to prevent FeB association.

The reaction between Fe_i and B can be described by the chemical reactions given in Sec. II Eq. (1). Out of Eq. (1) (solution of the rate-equation), the time dependent relative interstitial iron content $[Fe_i]_{relative}$ is only dependent on the association rate k_A and the dissociation rate k_D,

$$[Fe_i]_{relative} = \frac{k_D + k_A \exp[-(k_D + k_A)\,t]}{k_D + k_A}. \tag{4}$$

At low illuminations, leading to injection densities below the crossover point, the recombination through Fe_i is more effective than through FeB and the dissociation rate decreases during the measurement. Consequently, a time independent analysis of k_D is more accurate.[8] For comparison between the time dependent determined k_D (Eq. (4)) and the steady state determined value $[Fe_i]_{relative,t\to\infty}$, we used the steady

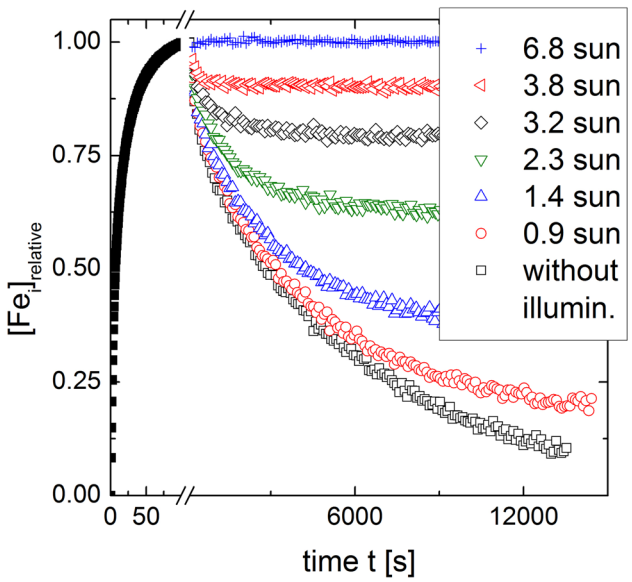

FIG. 6. Time dependent relative interstitial iron content of sample B at different illumination intensities.

state $[Fe_i]_{relative}$ value $[Fe_i]_{relative,t\to\infty} = \frac{k_D}{k_D+k_A}$. With the assumption that the association rate k_A keeps constant during illumination, the deviation between k_D determined by Eq. (4) and the steady state approach differs by $\leq 10\%$. The illumination dependent dissociation rate k_D as a function of the carrier generation rate G is depicted in Fig. 7. The carrier generation rate G at 1 sun was calculated using $G_{1\ sun} = 2.1 \times 10^{17}\,cm^{-2}\,s^{-1}/d$, where d is the (effective) sample thickness.[8] The dissociation rate k_D is described according to Geerligs *et al.*[8] by the quadratic function $k_D = K \cdot G^2/[FeB]$.[2] Thereby, the FeB concentration [FeB] equals the $[Fe_i]$ value given in Table I. The quadratic dependence of k_D indicates a two electron capture process involved in FeB dissociation.[5,8] In this work, the determined prefactor $K = 4.2 \times 10^{-17}$ s is two orders of magnitudes smaller than the value obtained by Geerligs *et al.*[8] which is $K = 5 \times 10^{-15}$ s. This deviation can be explained by the τ_{other} value of the samples used in this investigation. τ_{other} describes further recombination channels (other impurities, lattice defects, surface recombination) and reduces the recombination per FeB pair. Hence, the dissociation rate k_D decreases with decreasing τ_{other}.[8] For comparable determination of the prefactor K, the recombination per FeB trap is the crucial value. Unfortunately, it is hard to determine the recombination per FeB trap if the FeB trap is not the limiting recombination center. Hence, measurements on samples with $\tau_{other} \gg \tau_{FeB}$ are necessary to determine the recombination per FeB trap and a comparable prefactor K. Otherwise (as in the present investigation), the determined K is underestimated.

Illumination dependent investigations on p-type silicon samples are proper to determine both, the association rate and the dissociation rate dependent on generation rate.

C. Interstitial iron concentration determination in co-doped n-type silicon

The investigations in illuminated p-type silicon show a decreasing amount of associated FeB pairs with increasing illumination induced charge carrier density (see Sec. V B). Hence, the existing electron density in the boron and phosphorus co-doped n-type silicon leads to an underestimated interstitial iron content $[Fe_i]$ due to the larger dissociation rate k_D. The increased k_D influences the steady state between FeB pairs and Fe_i (similar to the increasing $[Fe_i]$ steady state in p-type silicon depicted in Fig. 6). With increasing (n-type) doping concentration the $[Fe_i]$ underestimation increases. In sample D, the interstitial iron content (determined by QSSPC lifetime measurement) in the co-doped p-type region was determined to $[Fe_i] = 6.9 \times 10^{12}\,cm^{-3}$ and in the co-doped n-type region to $[Fe_i] = 4.5 \times 10^{11}\,cm^{-3}$. The underestimated $[Fe_i]$ in n-type region does not influence the acceptor-dopant concentration determination by lifetime measurements (discussed in Sec. V D) because the association reaction is only dependent on the Fe_i diffusion[2] and not on the absolute $[Fe_i]$ value.

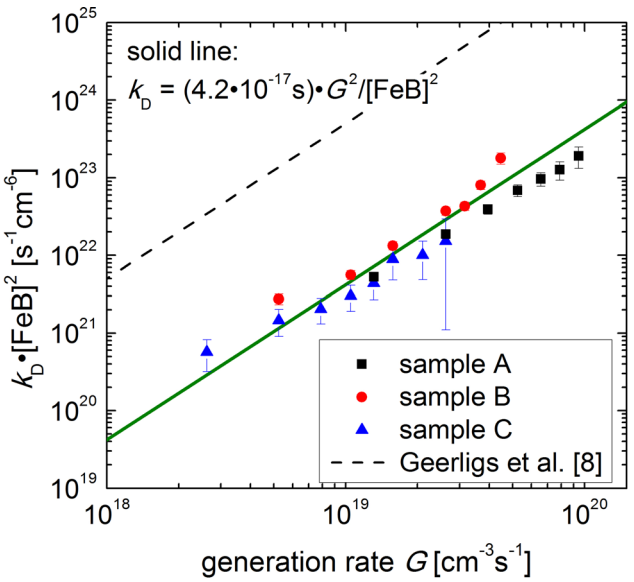

FIG. 7. FeB pair dissociation rate plotted as $k_D \cdot [FeB]^2$ over the light induced generation rate G. The solid line shows the quadratic dependence. The experimental results from Geerligs *et al.*[8] are depicted by a dashed line.

D. Acceptor density determination in co-doped n-type silicon

FeB association was observed in boron and phosphorus co-doped n-type silicon. Hence, acceptor dopant concentration determination out of the association kinetics[28,29] of the FeB pairs should be possible. An exponential fit to the reciprocal charge carrier lifetime values delivers the association time constant τ_{assoc} and the acceptor- (in this case boron) doping concentration N_A is calculated with[28,30]

$$N_A = \frac{\varepsilon\varepsilon_0 k_B}{q^2}\frac{T}{\tau_{assoc} D_0(T)} = \frac{5.7 \cdot 10^5}{\tau_{assoc}} T \exp\left[\frac{E_m}{k_B T}\right] cm^{-3}. \quad (5)$$

ε is the relative permittivity of silicon, ε_0 the dielectric constant, q the elementary charge and E_m the migration energy. This formula is established to determine the acceptor-doping concentration in p-type silicon.[24,31]

The migration energy of interstitial iron in p-type silicon (Fe_i^+) was determined to $E_{m,Fe_i^+} = 0.66\,eV$.[30] FeB pairing in co-doped n-type material occurs in the introduced model due to the permanent charge state change of the Fe_i. Hence, the charge state of Fe_i changes to predominantly *neutral* (with increasing dissociation rate) and the migration energy should increase up to $E_{m,Fe_i^0} = 0.8\,eV$ (migration energy for Fe_i^0 determined in n-type silicon).[7] To determine the association rate and therefore the acceptor dopant concentration, the dissociation rate and the migration energy of the investigated sample have to be known. Dissociation rate for a defined resistivity (charge carrier density) can be determined out of the dissociation rates in illuminated p-type silicon (Fig. 7). The electrons in p-type silicon generated by illumination have a similar effect as the electron density in co-doped n-type silicon. The generation rate can be calculated into an excess charge carrier density and into a Fermi level position. To investigate the dependence of E_{m,Fe_i^0} for different Fermi level positions in co-doped n-type silicon, a larger set of samples with constant resistivity is needed.

The acceptor dopant concentration of sample D was determined as follows. The total iron concentration, assumed

to be equal to the p-type area, was used to calculate the time dependent relative iron concentration and fit Eq. (4) to the experimental data. This procedure has the advantage that the dissociation rate follows out of the fit. The calculated acceptor doping concentration was compared with the theoretical value determined via Scheil equation[32] to determine the E_{m,Fe_i^0} value. For sample D the migration energy in the measured co-doped n-type region was determined to $E_{m,Fe_i^0} = 0.71\,\text{eV}$.

Fig. 8 depicts the theoretical boron (B) and phosphor (P) doping concentration calculated via Scheil equation, the net-doping (|B-P|) calculated out of the results of the Scheil equation, the measured resistivity at $x = 1\,\text{cm}$ and the determined boron concentration via lifetime measurement. The resistivity was determined with a 4-point-probe measurement and afterwards converted into the doping concentration using the charge carrier mobility model from Klaassen.[33,34] The values of the charge carrier density, needed for the charge carrier mobility calculation, were taken from the theoretical dopant densities from Scheil equation with the segregation coefficients of boron ($S_B = 0.8$) and phosphorus ($S_P = 0.35$).[35] The deviations from the calculated dopant density (dashed line in Fig. 8) and the measured dopant density (squares in Fig. 8) in p-type silicon are due to non-equilibrium with care of the industrial crystallisation. Hence, a deviation from Scheil equation, which is valid for the equilibrium case, is expected. Dopant concentration in the co-doped n-type region was calculated using Eq. (5).

The gray vertical dashed line (Fig. 8) depicts the position at which the n-type resistivity of 10 Ωcm ($y \approx 7.1\,\text{cm}$) is reached. At this point, the dissociation rate predominates the process in sample D and all FeB pairs are instable and no FeB pairing occurs. The stability region of the FeB pairs in co-doped n-type silicon should also be influenced by the boron (or other acceptors) and phosphorus concentration and is the aim of further investigations.

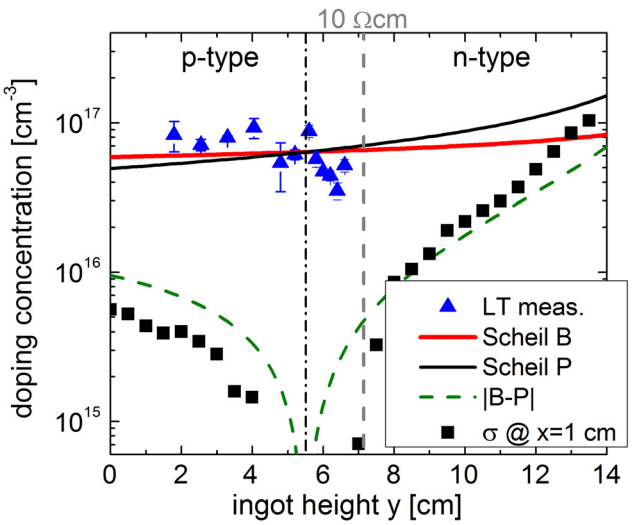

FIG. 8. Calculated (continuous lines) and measured (triangles) boron-doping concentration. The net-doping concentration from Scheil equation is depicted with the dashed line. For comparison, the measured resistivity was converted into a doping density and is depicted as squares.

VI. SUMMARY

The kinetics of iron-boron (FeB) pair association and dissociation are investigated under illumination in p-type silicon and in boron- and phosphorus-doped n-type silicon. Charge carrier lifetime change due to FeB association and dissociation in co-doped n-type silicon and illuminated p-type silicon was detected. The experimental findings are not explainable with the model from Kimerling and Benton.[5] Hence, a dynamic approach, based on the charge carrier capture and emission of the interstitial iron (Fe_i) trap level, was introduced. The recombination process leads to a dynamic recharging of the interstitial iron from neutral to single positively charged. While Fe_i is positively charged, FeB association becomes possible.

FeB pairing kinetics were used to determine the boron doping concentration in the n-type region of a boron and phosphorus co-doped silicon sample. Because of the charge state change of the Fe_i, the migration energy of Fe_i increases. The migration energy for the co-doped n-type silicon sample was, after comparison with the calculated doping concentration via Scheil equation, determined to $E_{m,Fe_i^0} = 0.71\,\text{eV}$.

ACKNOWLEDGMENTS

Funding of this work by the Federal Ministry of Economics and Technology of Germany under contract numbers KF2794102AG2 and KF 2020409AG2 (IKOSI) is acknowledged. The authors thank J. D. Murphy, F. Kirscht, and A. Lawerenz for helpful discussions.

[1]C. B. Collins and R. O. Carlson, Phys. Rev. **108**, 1409 (1957).
[2]A. A. Istratov, H. Hieslmair, and E. R. Weber, Appl. Phys. A **69**, 13 (1999).
[3]W. H. Shepherd and J. A. Turner, J. Phys. Chem. Solids **23**, 1697 (1962).
[4]S. Rein and S. W. Glunz, J. Appl. Phys. **98**, 113711 (2005).
[5]L. C. Kimerling and J. L. Benton, Physica B+C **116**, 297 (1983).
[6]K. Graff and H. Pieper, J. Electrochem. Soc. **128**, 669 (1981).
[7]H. Takahashi, M. Suezawa, and K. Sumino, Phys. Rev. B **46**, 1882 (1992).
[8]L. J. Geerligs and D. Macdonald, Appl. Phys. Lett. **85**, 5227 (2004).
[9]D. V. Lang and L. C. Kimerling, Phys. Rev. Lett. **33**, 489 (1974).
[10]J. D. Weeks, J. C. Tully, and L. C. Kimerling, Phys. Rev. B **12**, 3286 (1975).
[11]H. Sumi, Phys. Rev. B **29**, 4616 (1984).
[12]C. Möller, A. Laades, and K. Lauer, Solid State Phenom. **205–206**, 265 (2013).
[13]J. D. Murphy and R. J. Falster, Phys. Status Solidi RRL **5**, 370 (2011).
[14]J. D. Murphy and R. J. Falster, J. Appl. Phys. **112**, 113506 (2012).
[15]A. Laades, M. Blech, M. Bahr, K. Lauer, and A. Lawerenz, Phys. Status Solidi C **8**, 763 (2011).
[16]N. D. Arora, J. R. Hauser, and D. J. Roulston, IEEE Trans. Electron Devices **29**, 292 (1982).
[17]DIN EN 50513 (VDE0126-18):2009–12; available at https://www.vde-verlag.de/normen/0126027/din-en-50513-vde-0126-18-2009-12.html.
[18]R. A. Sinton and A. Cuevas, Appl. Phys. Lett. **69**, 2510 (1996).
[19]K. Lauer, A. Laades, H. Übensee, H. Metzner, and A. Lawerenz, J. Appl. Phys. **104**, 104503 (2008).
[20]R. Brendel, Appl. Phys. A **60**, 523 (1995).
[21]G. Zoth and W. Bergholz, J. Appl. Phys. **67**, 6764 (1990).
[22]H. Conzelmann, K. Graff, and E. R. Weber, Appl. Phys. A **30**, 169 (1983).
[23]H. Väinölä, E. Saarnilehto, M. Yli-Koski, A. Haarahiltunen, J. Sinkkonen, G. Berenyi, and T. Pavelka, Appl. Phys. Lett. **87**, 032109 (2005).
[24]D. Macdonald, L. J. Geerligs, and A. Azzizi, J. Appl. Phys. **95**, 1021 (2004).
[25]D. Macdonald, T. Roth, P. N. K. Deenapanray, K. Bothe, P. Pohl, and J. Schmidt, J. Appl. Phys. **98**, 083509 (2005).
[26]S. Rein, *Lifetime Spectroscopy: A Method of Defect Characterization in Silicon for Photovoltaic Applications* (Springer, Berlin, 2005), p. 43–44.

[27]D. Macdonald, T. Roth, P. N. K. Deenapanray, T. Trupke, and R. A. Bardos, Appl. Phys. Lett. **89**, 142107 (2006).
[28]H. Reiss, C. S. Fuller, and F. J. Morin, Bell Syst. Tech. J. **35**, 535 (1956).
[29]E. M. Pell and F. S. Ham, J. Appl. Phys. **32**, 1052 (1961).
[30]J. Tan, D. Macdonald, F. Rougieux, and A. Cuevas, Semicond. Sci. Technol. **26**, 055019 (2011).
[31]D. Macdonald, A. Cuevas, and L. J. Geerligs, Appl. Phys. Lett. **92**, 202119 (2008).
[32]E. Scheil, Z. Metallk. **34**, 70 (1942).
[33]D. B. M. Klaassen, Solid-State Electron. **35**, 953 (1992).
[34]D. B. M. Klaassen, Solid-State Electron. **35**, 961 (1992).
[35]F. Shimura, *Semiconductor Silicon Crystal Technology* (Academic Press, 1989), p. 149.